Analysis of stable components in the extended-range forecast for the coming 10–30 days in winter 2010 and 2011*

Wang Kuo(王 阔)[a], Feng Guo-Lin(封国林)[b]†, Zeng Yu-Xing(曾宇星)[a], and Wang Xu-Jia(汪栩加)[a]

[a] College of Atmospheric Sciences, Lanzhou University, Lanzhou 730000, China
[b] Laboratory for Climate Studies, National Climate Center, China Meteorological Administration, Beijing 100081, China

(Received 29 March 2013; revised manuscript received 10 May 2013)

In this paper we try to extract stable components in the extended-range forecast for the coming 10–30 days by using empirical orthogonal function (EOF) analysis, similarity coefficient, and some other methods based on the National Center for Environmental Prediction (NCEP)/National Center for Atmospheric Research (NCAR) reanalysis daily data. The comparisons of the coefficient of variance of climatological background field and truth data in winter between 2010 and 2011 are made. The method of extracting stable components and climatological background field can be helpful to increase forecasting skill. The forecasting skill improvement of air temperature is better than geopotential height at 500 hPa. Moreover, this method improves the predictability better in the Pacific Ocean. In China, the forecast in winter in Northeast China is more uncertain than in the other parts.

Keywords: stable components, climatological background, coefficient of variance

PACS: 92.60.Wc **DOI:** 10.1088/1674-1056/22/12/129202

1. Introduction

In recent years, the standards of the extended-range forecast in the coming 10–30 days have been improving greatly. Because the atmosphere is a forced dissipative nonlinear system, its predictability is sensitive to initial condition. It has long been recognized that the upper limit of weather predictability for the synoptic and larger scales is about 2 weeks.[1–6] However, it is well established that some components in the climate system are more predictable than others. For instance, large-scale structures tend to be more predictable than small-scale structures and numerical evidence supports the hypothesis that the climate state is predictable beyond 2 weeks.[7,8] Studies show that some low-frequency atmosphere system can be observed. For example, as the Madden–Julian oscillation (MJO) has been found,[9,10] research results support that MJO influences the weather significantly in China.[11–13] These studies strengthen our confidence to improve the extended-range forecast in the coming 10–30 days.

The extended-range forecast in the coming 10–30 days is gradually becoming a hot study direction in weather forecasting. Chen *et at.*,[14] and Ding and Li[15] introduced a new approach using the nonlinear local Lyapunov exponent (NLLE) to study the atmospheric predictability from the view of nonlinear error growth dynamics. The spatiotemporal distributions of predictability limit of monthly and seasonal mean geopotential height and temperature fields were investigated.[16,17] Moreover, Mu[18] established a novel concept of nonlinear singular vector (NSV) and nonlinear singular vector value (NSVA) and improved the technique of conditional nonlinear optimal perturbations (CNOPs). These study results were used widely in the study of predictability, ensemble forecast, and many other fields.[19,20]

The interannual variability of a climate mean consists of both climate signal and noise. The climate signals are those variations forced by the slowly varying anomalous boundary conditions external to the climate system.[21–24] A climate anomaly may display a certain degree of predictability if the percentage of climate signal in its total variability is large enough to overcome the destructive effect of the noise.[25] Many observations and studies showed that there is a strong relationship between the stable component and atmospheric oscillation,[26–29] and the stable components can be forecasted objectively on a 10–30 day time scale.[30–34] Therefore, some work extracted stable components in the extended-range forecast for the coming 10–30 days by using empirical orthogonal function (EOF) analysis and some other methods during the snow storm event in the winter 2010 and 2011.[35–37] The stable components in the extended-range forecast for the coming 10–30 days can be divided objectively into two parts, i.e., climatic stable components and abnormal stable components, by analyzing the contribution rate, similarity coefficient, etc. We combine climatic stable components and low-pass filter components to obtain the climatological background field and to investigate the 10–30 day component background. In this paper, the coefficient of variance is calculated to examine the predictability between true atmosphere and climatological back-

*Project supported by the National Basic Research Program of China (Grant No. 2013CB430204), the National Natural Science Foundation of China (Grant Nos. 40930952 and 41105070), and the State Key Development Program for Basic Research of China (Grant No. 2012CB955902).

†Corresponding author. E-mail: fenggl@cma.gov.cn

© 2013 Chinese Physical Society and IOP Publishing Ltd

ground field in the last two winters. These results can deepen our understanding of the predictability of the extended range forecast for the coming 10–30 days and provide a new way to think and solve the problem of the extended range forecast for the coming 10–30 days.

2. Data and method

2.1. Data

This study is based on the data reanalyzed by the National Center for Environmental Prediction/ National Center for Atmospheric Research (NCEP/NCAR)[38] for the period January 1980–April 2012. The dataset has a $2.5^\circ \times 2.5^\circ$ horizontal resolution and extends from 1000 hPa to 10 hPa, with 17 vertical pressure levels. The data of February 29 in leap years are omitted to keep it consistent.

2.2. Method

In this paper the components in the extended-range forecast for the coming 10–30 days are extracted by the Butterworth Band-pass Filter on a monthly timescale. There we just extract stable components in the extended-range forecast for the coming 10–30 days in December of 2010 for example. The basic function of climate state can be extracted by EOF analysis based on the NCEP/NCAR reanalysis daily data of geopotential height from 1981 to 2010 in December from the following equation:

$$X_{m\times n} = V_{m\times m} T_{m\times n}, \tag{1}$$

where $X_{m\times n}$ is the sequence of meteorological elements, $V_{m\times m}$ is the space characteristic vector, and $T_{m\times n}$ is time coefficient. Then we calculate the daily data of geopotential height in December of 2010 by the Butterworth Band-pass Filter. Based on Eq. (1), contribution rate can be obtained by combining the space characteristic vectors of EOF and the corresponding time coefficients; the time coefficients can be calculated from the following equation:

$$T = V'X. \tag{2}$$

The contribution rate is used to check how to influence the original field and explain the elements which influence this weather process in view of 10–30 days. When the explained variance of one component stays at the top twenty for more than fifteen days in one month, we define this component as a stable component in the extended-range forecast for the coming 10–30 days.

There are three big circulation systems at 500 hPa: subtropical high system in low latitudes, westerly belt system in middle latitudes, and polar vortex system in high latitude. The active degrees of these three circulation systems are different in different seasons. For example, the westerly belt system shows three strong troughs in winter, but four weak troughs in summer instead. The anomalies of three big circulation systems can lead to the anomaly of atmospheric circulation. Experiences show that atmospheric circulations are different in different seasons and different sectors. If the daily contribution rates of the top 50 eigenvectors in December 2010 correspond to these in climate perfectly, the change of weather system would be similar to its historical change. Because they are different (Fig. 1), many extreme weather events happen every year. Therefore, it is an interesting thing to study the change of explained variances of eigenvectors.

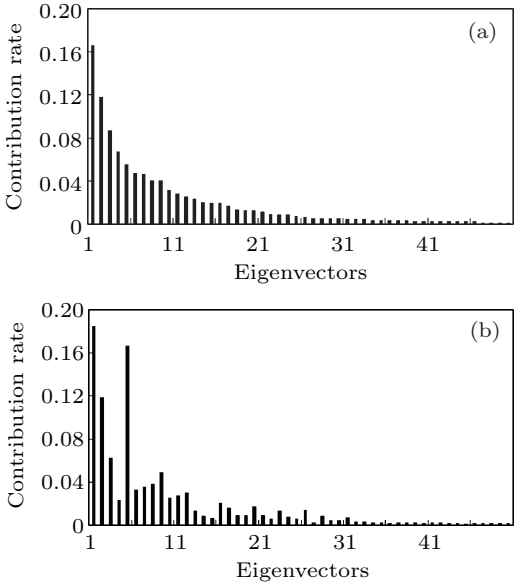


Fig. 1. December contribution rate: (a) climate and (b) 2010.

Y is defined as a threshold to separate the climatic stable component from the abnormal stable component. One stable component, whose sequence of explained variance in climate minus its sequence of explained variance of a case is less than Y in absolute value, is called a climatic stable component. Moreover, one stable component, whose sequence of explained variance in climate minus its sequence of explained variance of a case is equal or more than Y in absolute value, is called an abnormal stable component. There we assign the numbers from one to fifteen to Y and obtain the corresponding climatic stable components. The similarity coefficient (Eq. (3)) between climatic stable components in 1981 to 2010 is calculated and the climatic stable component of a case.

$$\cos(\theta) = \frac{\sum_{i=1}^{m} x_i y_i}{\sqrt{\sum_{i=1}^{m} x_i^2}\sqrt{\sum_{i=1}^{m} y_i^2}}, \tag{3}$$

where $\cos(\theta)$ represents the similarity coefficient, x and y are different metrorological elements, and m is sample size.

The flowchart of the objective separation of stable components is shown in Fig. 2. First, according to the 1980–2010

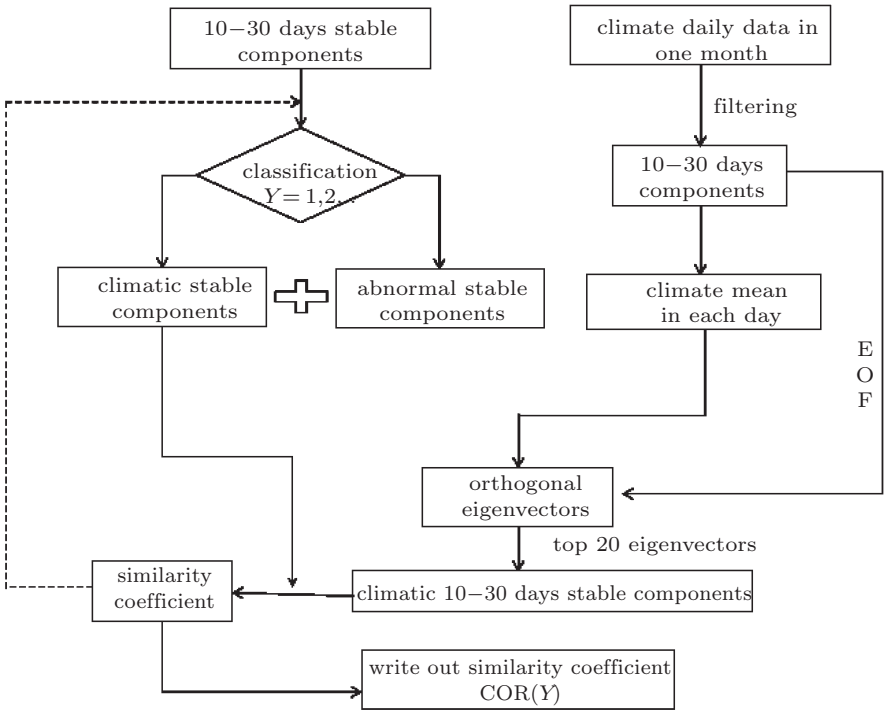


Fig. 2. Flowchart of the objective separation of stable components.

NCEP/NCAR data in December, the 10–30 days components are obtained. Subsequently, climatic mean 10–30 day components in each day are multiplied by orthogonal eigenvectors. The top 20 eigenvectors are selected to obtain climatic 10–30 day stable components, and the similarity coefficient is calculated with climatic stable components. We consider that when the similarity coefficient reaches extremum, Y is the right threshold that we want (Fig. 3). At this time, the climatic stable components and abnormal stable components can be ascertained objectively. For example in this case the geopotential height data in December 2010 at 500-hPa level, 2 is a reasonable threshold for Y. We combine climatic stable components and low-pass filter components to obtain climatological background field.

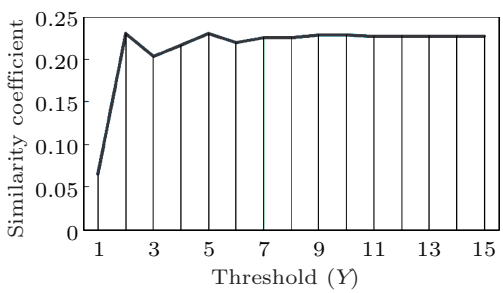


Fig. 3. Similarity coefficient between climatic 10–30 day stable component and climatic stable component when the threshold is in a range from 1–15.

The standard deviation is

$$S_x = \sqrt{\frac{1}{n}\sum_{t=1}^{n}(x_t - \bar{x})^2}, \tag{4}$$

where x is the meteorological time series; $\bar{x}$ is average; n is sample size. Standard deviation represents the average level of the variable change around the average. So it can reflect the level of difficulty in predicting the variable. Of course, it is easier to predict a variable with lower S_x than with higher S_x. However, if there are two variables with different magnitudes, each changes according to its own percentage, we can obtain that their standard deviations are not equal. The larger magnitude variable has a higher standard deviation and the smaller magnitude variable has a lower standard deviation. In order to avoid this relative error and to compare the 500-hPa geopotential height and the climatological background field, we calculate their coefficient of variance (CV) from the following formula:

$$\mathrm{CV} = \frac{1}{\bar{x}}\sqrt{\frac{1}{n}\sum_{t=1}^{n}(x_t - \bar{x})^2} \tag{5}$$

to compare their predictabilities.

3. Geopotential field and temperature field at 500 hPa in winter 2010

3.1. Geopotential field at 500 hPa

3.1.1. The CV analysis of truth field

Figure 4 shows the CVs of truth field at 500-hPa level in the Northern Hemisphere in winter 2010. The CVs reach their minima in the equator and increase along the direction of latitude increasing. It is in accordance with Li and Wang's studies.[39] In December 2010, the CVs are below 0.005 in south of 20° north latitude. They are lower in Southwest China

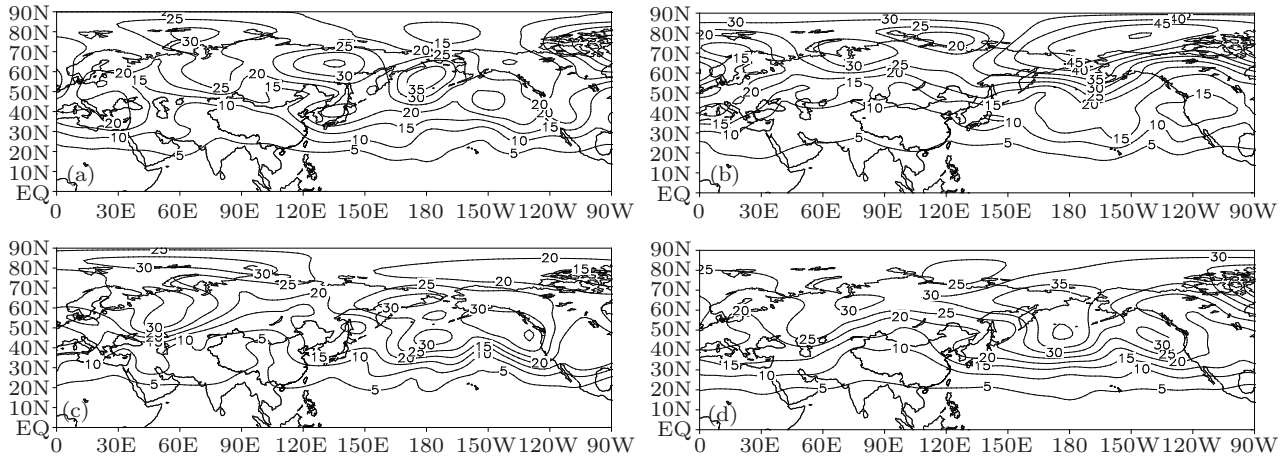


Fig. 4. The CVs of geopotential truth field at 500-hPa level in the Northern Hemisphere in (a) December 2010, (b) January 2011, (c) February 2011, and (d) Winter 2010. December, January, and February (DJF) ($\times 10^{-3}$).

and higher in Northeast China. There is a closed-isoline in the Sea of Japan, with values exceeding 0.025. In January 2011, the CVs in China are similar except in Northeast China. The isolines become dense in high latitudes. In February 2011, they change a little but turn a closed-isoline in the North Pacific Ocean. The CV isolines become dense in mid-latitudes of the Pacific Ocean and the uncertainty of prediction increases. According to Fig. 4(d), the CVs are higher in Northeast China than in the other parts of China in winter 2010. Moreover, the isolines are dense in the North Pacific Ocean.

3.1.2. The CV analysis of climatological background field

From the CVs of geopotential climatological background field at 500-hPa level in the Northern Hemisphere in Fig. 5, we can obtain the information similar to that in Fig. 4. The CVs of climatological background field in Eurasia during December 2010 have two closed-isolines, and the west one is stronger than the other. In January 2011, there is a high closed-isoline in Northeast China and the Sea of Japan, while the 0.005 isoline moves toward north which means that in this section the forecast skills are higher than December 2010. From Fig. 5 we can see that in high latitudes the CVs are higher than those in low latitudes, at the same time they show zonal distribution. In winter 2010 (Fig. 5(d)), the CVs are higher in Northeast China than in the other parts of China too. Especially, a comparison of Fig. 4 with Fig. 5 shows that the CVs of climatological background field are obviously less than the CVs of the truth field in both Asia and the Pacific Ocean. It means that the climatological background field is easier to predict than the truth field at 500-hPa level. Therefore, the method of extracting stable components and obtaining climatological background field is helpful to increase the forecast skills. Moreover, the values in both truth field and climatological background field are higher in Northeast China than in the other parts. We may explain that in China the forecast of geopotential field at 500 hPa in winter in Northeast China is more uncertain.

3.2. Temperature field at 500 hPa

3.2.1. The CV analysis of truth field

From the CVs of the truth field at 500-hPa level in the Northern Hemisphere (Fig. 6) we can see that the CVs are very low in low-latitudes and increase along the direction of increasing latitude. The CVs are low in Southwest China while high in Northeast China. In January 2011, the CVs

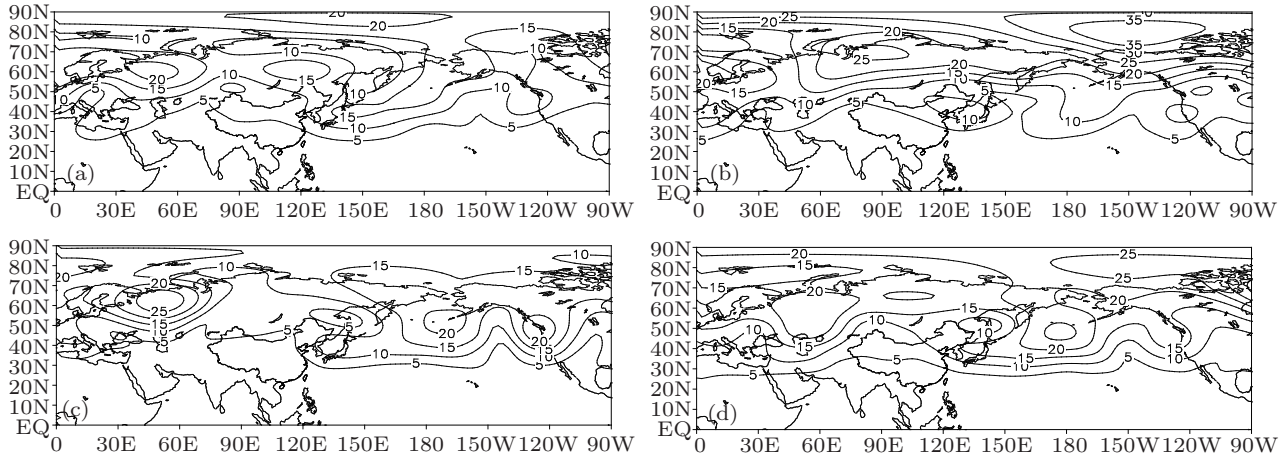


Fig. 5. The CVs of geopotential climatological background field at 500-hPa level in the Northern Hemisphere in (a) December 2010, (b) January 2011, (c) February 2011, and (d) Winter 2010. (DJF) ($\times 10^{-3}$).

of the truth field are flat south of 40° north latitude. They are lower in Southwest China while higher in Northeast China. With the time going on, there is a high closed-isoline which influences most of the Northwest Pacific Ocean at 500 hPa in February 2011. The 0.015 isoline moves to south in China which makes CVs in Northeast China and North China higher. Figure 6 shows that there is a high closed-isoline exceeding 0.025 in the North Pacific Ocean in winter 2010. The CVs of temperature truth field of China reach their maxima in Northeast China.

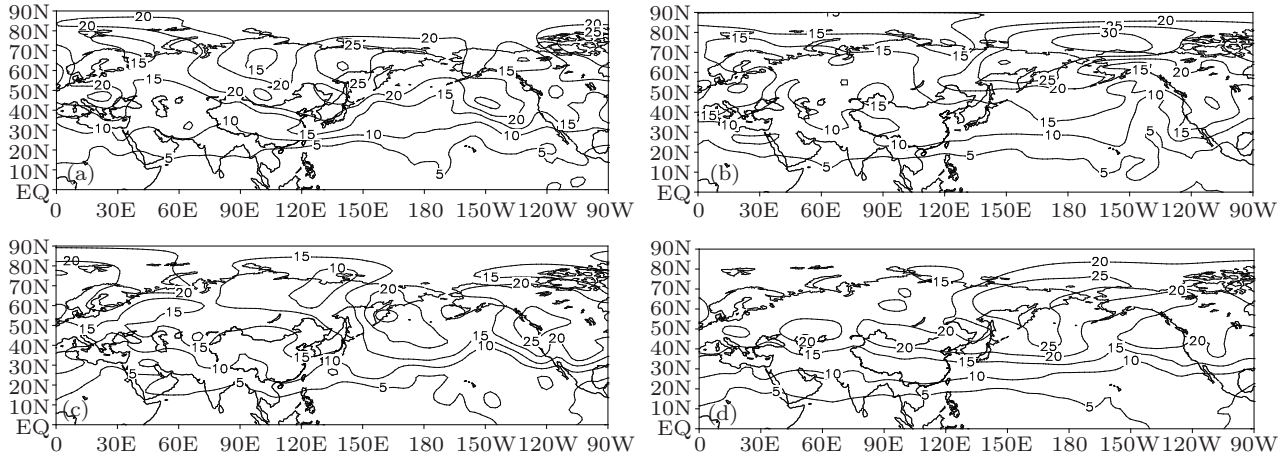


Fig. 6. The CVs of temperature truth field at 500-hPa level in the Northern Hemisphere in (a) December 2010, (b) January 2011, (c) February 2011, and (d) Winter 2010. (DJF) ($\times 10^{-3}$).

3.2.2. The CV analysis of climatological background field

Figure 7 shows the CVs of temperature climatological background field at 500-hPa level in the Northern Hemisphere. It displays the zonal distribution in December 2010 and changes little in the south of 20° N. The isolines become dense in the section of juncture of Eurasia and the Pacific Ocean. In January 2011 there are two high closed-isolines in Northeast China and Okhotsk, which influence the change of temperature at 500 hPa together. The CVs of climatological background field at 500 hPa are sparse in February 2011 and show a high closed-isoline in the Central Pacific Ocean which influences East China, especially some coastal areas.

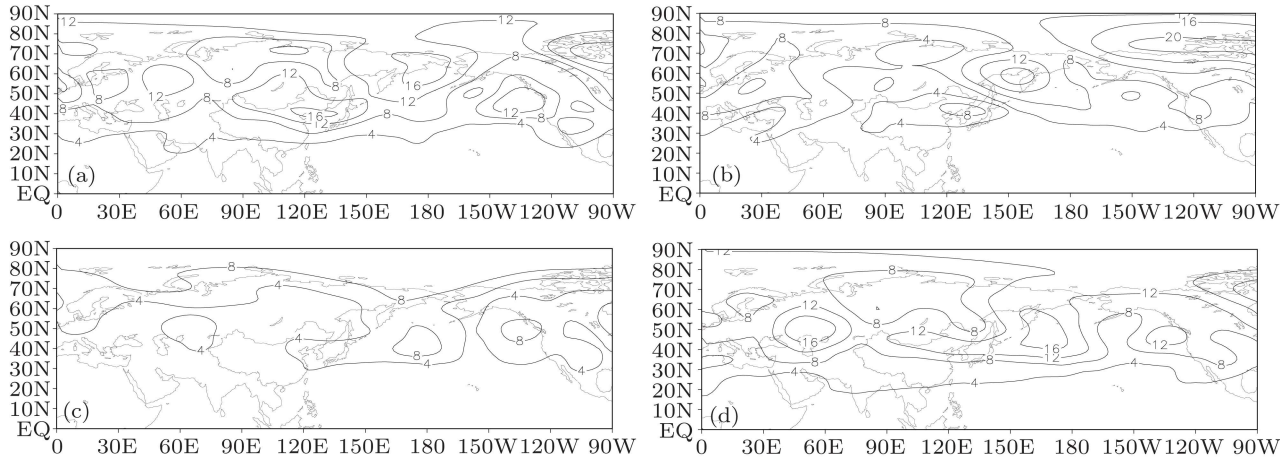


Fig. 7. The CVs of temperature climatological background field at 500-hPa level in the Northern Hemisphere in (a) December 2010, (b) January 2011, (c) February 2011, and (d) Winter 2010. (DJF) ($\times 10^{-3}$).

From the CVs of temperature climatological background field at 500-hPa level in the Northern Hemisphere in winter 2010 we can see that there is a strong high center in the Northwest Pacific Ocean which makes the isolines in Northeast China dense. We consider that the predictability in Northeast China is influenced mainly by the Northwest Pacific Ocean at 500-hPa level. Comparing Fig. 6 with Fig. 7, the CVs of temperature climatological background field are more stable than that of the truth field.

4. Geopotential field and temperature field at 500 hPa in winter 2011

4.1. Geopotential field at 500 hPa

4.1.1. The CV analysis of truth field

Figure 8 shows the CVs of geopotential truth field at 500-hPa level in the Northern Hemisphere in winter 2011. The

predictability in low latitudes is better than in other latitudes. In December 2011 and February 2012, there is a high closed-isoline exceeding 0.030 in the East Pacific Ocean. While in January 2012 the high closed-isoline appears in the Aleutian area, which influences East Siberia obviously. From winter 2011 we can see that there are two closed-isolines in the North Pacific Ocean and the East Pacific Ocean and the coefficients of variance in the West Pacific Ocean are sparse. The coefficients of variance in Northeast China are higher than in the other parts in China, which means that the predictability limit in Northeast China is higher too. Comparing with Fig. 4, the source region of the weather system influencing the distribution of coefficients of variance in China can be distinguished as two parts by time sequence: In early winter, the source region is in Siberia of North Eurasia, while in later winter, the source region is the Pacific Ocean.

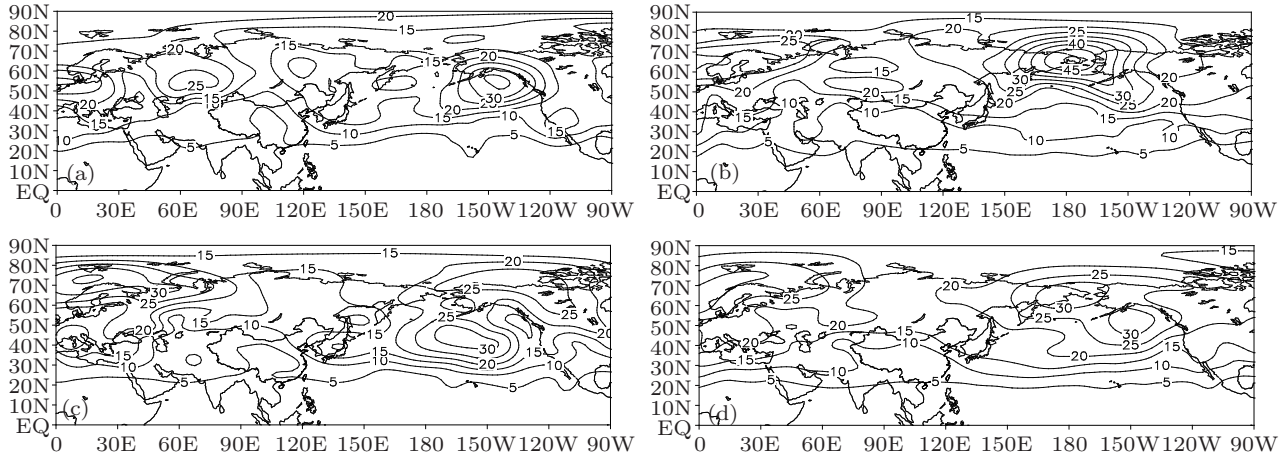


Fig. 8. The CVs of geopotential truth field at 500-hPa level in the Northern Hemisphere in (a) December 2011, (b) January 2012, (c) February 2012, and (d) Winter 2011. (DJF) ($\times 10^{-3}$).

4.1.2. The CV analysis of climatological background field

Comparing Fig. 8 with Fig. 9, we can see that the CVs of climatological background field we extracted are lower than those of the truth field in the same areas. Moreover, the patterns in two fields are very similar, which means that the climatological background field can grasp the main circulation systems in the truth field. Although just calculating low-pass filtering may also show some improvement, it is not clear whether separating climate signal from noise can lose some useful information. Obviously, the method we put forward is better than the simple low-pass filtering.

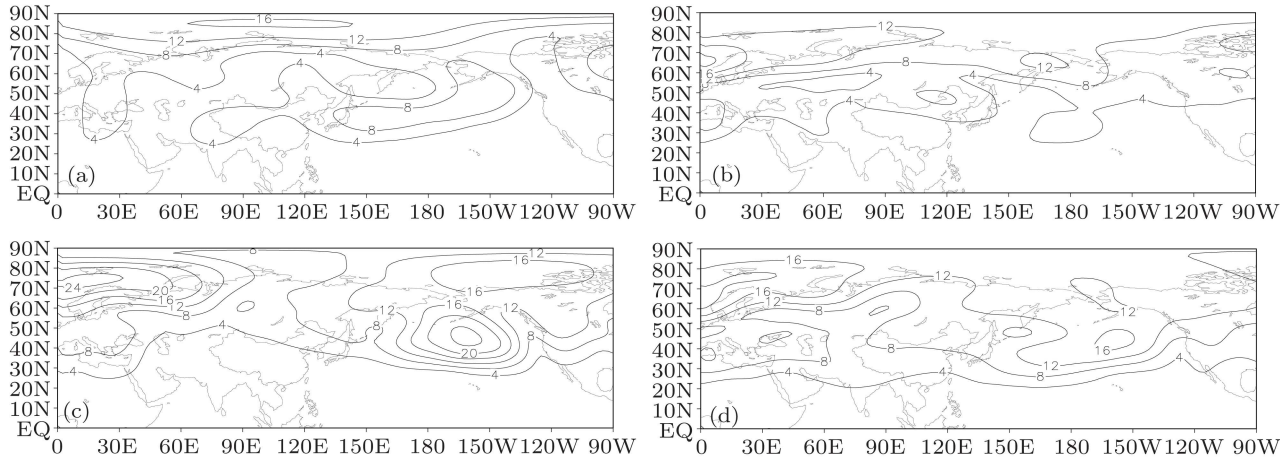


Fig. 9. The CVs of geopotential climatological background field at 500-hPa level in the Northern Hemisphere in (a) December 2011. (b) January 2012. (c) February 2012 , and (d) Winter 2011. (DJF) ($\times 10^{-3}$).

4.2. Temperature field at 500 hPa

4.2.1. The CV analysis of truth field

Figure 10 shows the CVs of temperature truth field at 500-hPa level in the Northern Hemisphere. In December 2011 and January 2012, high closed-isolines are in the North Pacific Ocean and the section of juncture of America and the Northeast Pacific Ocean. Then the high closed-isoline moves to the Center Pacific Ocean in February 2012. The CVs of the truth field in winter 2011 (Fig. 10(d)) shows that they change little in the same latitudes. The predictability of North China is lower than in the other parts, this phenomenon is similar to that in winter 2010.

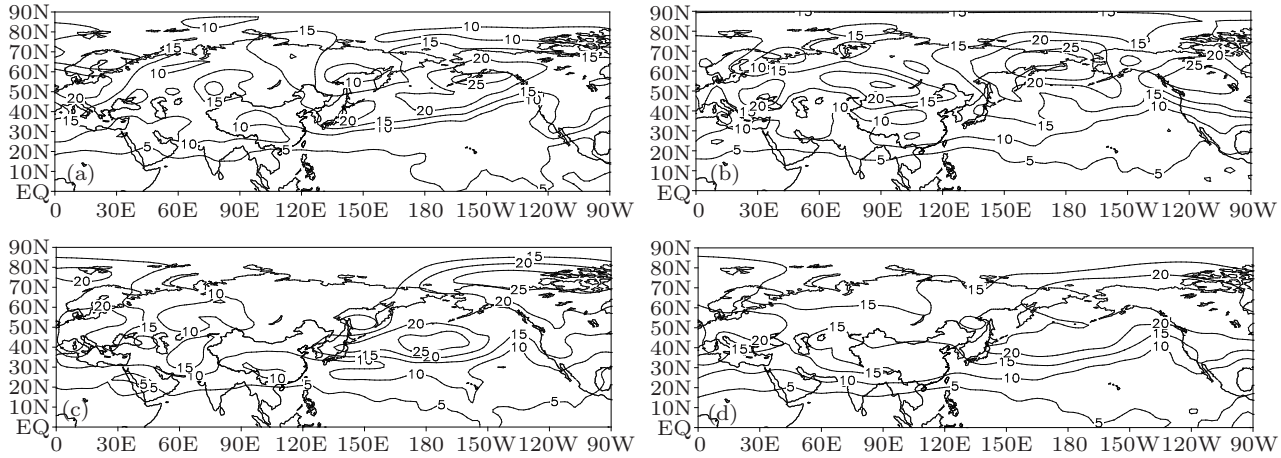


Fig. 10. The CVs of temperature truth field at 500-hPa level in the Northern Hemisphere in (a) December 2011, (b) January 2012, (c) February 2012, and (d) Winter 2011. (DJF) ($\times 10^{-3}$).

4.2.2. The CV analysis of climatological background field

Figure 11 shows the CVs of temperature climatological background field at 500-hPa level in the Northern Hemisphere. Comparing with Fig. 7, it is obvious to find that the CVs are very sparse and different from month to month. The CVs in China become lower and lower with the time going on and they are almost below 0.004 in February 2012. The predictability is better south of 30° north latitude with the CVs below 0.005 in winter. Moreover, Fig. 11 shows the temperature CVs in Northeast China are mainly influenced by the North Pacific Ocean and the predictability in the East Pacific Ocean is better than that in the West Pacific Ocean.

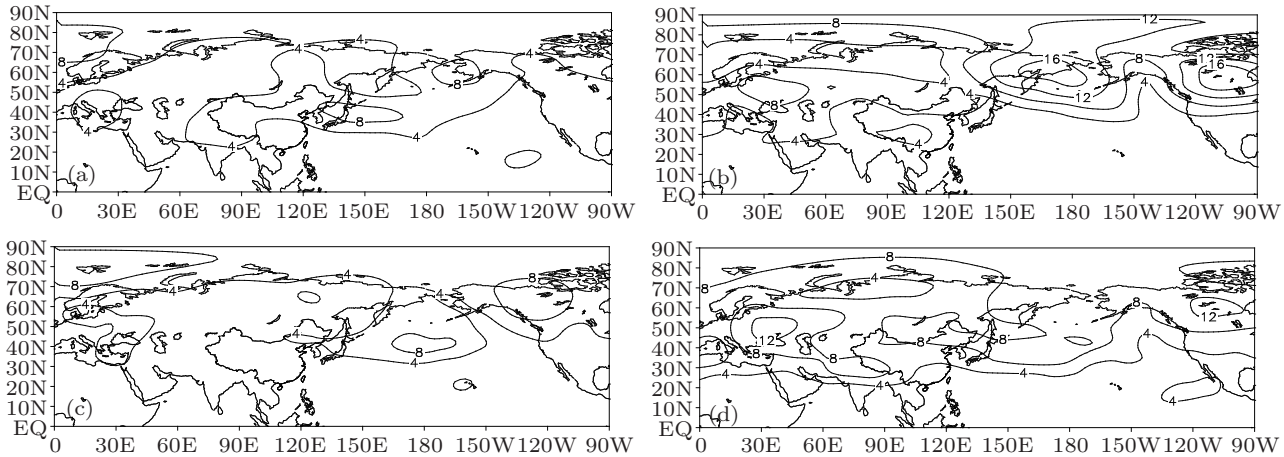


Fig. 11. The CVs of temperature climatological background field at 500-hPa level in the Northern Hemisphere in (a) December 2011, (b) January 2012, (c) February 2012, and (d) Winter 2011. (DJF) ($\times 10^{-3}$).

5. Conclusion and discussion

In this paper, we try to extract the stable components in the extended-range forecast for the coming 10–30 days by using empirical orthogonal function analysis, similarity coefficient and some other methods based on the NCEP/NCAR reanalyzed daily data. The CVs of climatological background field and truth field in the winter 2010 and 2011 are compared to obtain some results.

The method of extracting stable components and climatological background field can be helpful to increase the forecasting skill. The improvement on air temperature is better than geopotential height at 500 hPa. It is meaningful for the extended-range forecast for the coming 10–30 days.

From the distribution of CVs in winter 2010 and 2011 we can see that the predictability decreases along the direction of increasing latitude. Moreover, this method improves the predictability obviously in the Pacific Ocean. The forecast in winter in Northeast China is more uncertain than in the other parts of China. The predictability of air temperature in Northeast China is influenced by the North Pacific Ocean mainly at 500 hPa.

In this paper a new method of separating climate signal from noise is developed to solve the difficulty in extended-range forecast for the coming 10–30 days based on some comprehensive studies. The results seem encouraging. However, the relevant studies need to be continued to combine this method with model results for the weather forecast. Moreover, how to combine with boundary conditions, for example,

ENSO, also needs to be investigated.

References

[1] Lorenz E N 1965 *Tellus* **17** 321
[2] Lorenz E N 1969 *J. Atmos. Sci.* **26** 636
[3] Xie T, Zou G H, William P, Kuang H L and Chen W 2010 *Chin. Phys. B* **19** 059201
[4] Jiang H, Yang X X, Lin M M, Shi Y R and Duan W S 2011 *Chin. Phys. B* **20** 019401
[5] Feng G L, Dai X G, Wang A H and Chou J F 2001 *Acta Phys. Sin.* **50** 606 (in Chinese)
[6] Zhang Z S, Gong Z Q, Zhi R, Feng G L and Hu J G 2011 *Chin. Phys. B* **20** 019201
[7] Shukla J 1981 *J. Atmos. Sci.* **38** 2547
[8] Shukla J 1998 *Science* **282** 728
[9] Madden R A and Julian P R 1971 *J. Atmos. Sci.* **28** 702
[10] Madden R A and Julian P R 1972 *J. Atmos. Sci.* **29** 1109
[11] Wang B and Liu F 2011 *J. Atmos. Sci.* **68** 2524
[12] Jia X, Chen L J, Ren F M and Li C Y 2011 *Adv. Atmos. Sci.* **28** 521
[13] Li C Y and Zhou Y P 1994 *Chin. J. Geophys.* **37** 213 (in Chinese)
[14] Chen B H, Li J P and Ding R Q 2006 *Sci. China Ser. D* **49** 1111
[15] Ding R Q and Li J P 2007 *Phys. Lett. A* **364** 396
[16] Ding R Q, Li J P and Ha K J 2008 *J. Geophys. Res.* **113** D24112
[17] Ding R Q, Li J P and Seo K H 2011 *Mon. Wea. Rev.* **139** 2421
[18] Mu M 2000 *Sci. China Ser. D* **43** 375
[19] Mu M, Duan W S, Xu H and Wang B 2006 *Adv. Atmos. Sci.* **6** 992
[20] Zhou F F and Mu M 2012 *Adv. Atmos. Sci.* **29** 705
[21] Yang S, Zhang Z, Kousky V E, Higgins R W, Yoo S H, Liang J and Fan Y 2008 *J. Climate* **21** 3755
[22] Qian Z H, Hu J G, Feng G L and Cao Y Z 2012 *Chin. Phys. B* **21** 109203
[23] Horel J D and Wallace J M 1981 *Mon. Wea. Rev.* **109** 813
[24] Blackmon M L, Geisler J E and Pitcher E J 1983 *J. Atmos. Sci.* **40** 1410
[25] Chen W Y and Van den Dool H M 1996 *J. Climate* **10** 1236
[26] Plaut G and Vautard R 1994 *J. Atmos. Sci.* **51** 210
[27] Li C Y and Pan J 2006 *Adv. Atmos. Sci.* **23** 925
[28] Wang X J, Zhi R, He W P and Gong Z Q 2012 *Chin. Phys. B* **21** 029201
[29] Gong Z Q, Wang X J, Zhi R and Feng A X 2011 *Chin. Phys. B* **20** 079201
[30] Blackmon M L, Lee Y H, Wallace J M and Hsu H H 1984 *J. Atmos. Sci.* **41** 981
[31] Barnett T P and Preisendorfer R 1987 *Mon. Wea. Rev.* **115** 1825
[32] DelSole T and Tippett M K 2008 *J. Atmos. Sci.* **65** 1666
[33] Chou J F 2011 *Advances in Meteorological Science and Technology* **1** 11 (in Chinese)
[34] Chou J F 2012 *Chin. J. Geophys.* **55** 1433 (in Chinese)
[35] Wang K, Feng G L, Sun S P and Zheng Z H 2012 *Acta Phys. Sin.* **61** 109201 (in Chinese)
[36] Wang K, Feng G L, Sun S P and Zheng Z H 2012 *Acta Phys. Sin.* **61** 209201 (in Chinese)
[37] Zheng Z H, Huang J P, Feng G L and Chou J F 2012 *Sci. China Earth Sci.* **56** 878
[38] Kalnay E and Coauthors 1996 *Meteor. Soc.* **77** 437
[39] Li F and Wang H J 2012 *Adv. Atmos. Sci.* **29** 441